Journal of Hydrology 503 (2013) 22–28

Contents lists available at ScienceDirect

Journal of Hydrology

journal homepage: www.elsevier.com/locate/jhydrol

Specific storage from sparse records of groundwater response to seismic waves

Attila J.B. Folnagy, James L. Osiensky, Daisuke Kobayashi *, Kenneth F. Sprenke

Department of Geological Sciences, University of Idaho, Moscow, ID 83844, USA

ARTICLE INFO

Article history:
Received 18 June 2013
Received in revised form 13 August 2013
Accepted 26 August 2013
Available online 31 August 2013
This manuscript was handled by Peter K. Kitanidis, Editor-in-Chief, with the assistance of Niklas Linde, Associate Editor

Keywords:
Specific storage
Rayleigh wave
Hydrogeophysics
Hydroseismicity
Groundwater

SUMMARY

Rayleigh waves from moderately large earthquakes produce, at all epicentral distances, significant groundwater fluctuations. The direct comparison of seismic Rayleigh waves and associated groundwater oscillations has previously been shown to be useful for evaluating the specific storage of aquifers. However, such methods require measuring water levels on a scale of seconds rather than the more typical scale of minutes employed in most well recorders. A new computation procedure is needed to deal with this sparse amount of water level data provided by the most data loggers relative to seismological data. We show that, given the transmissivity of a confined uniformly porous aquifer, a single water level deflection measurement, if normalized to an appropriately filtered power spectrum of the associated Rayleigh wave motion, can provide a rough but unbiased estimate of specific storage. Given a sufficient number of such discrete observations, specific storage can be computed to the same accuracy as can be found from continuous well records. The precision of the algorithm is strongly dependent on the number of water level measurements available during the passage of Rayleigh waves. However, because each water level measurement is treated independently, data from multiple earthquakes can be combined to ensure a low computational error. Of course, the overall accuracy of the method depends not only on the computation procedure but also on the fit of the aquifer to the initial assumptions and on the extent to which the aquifer transmissivity is known.

1. Introduction

Earthquakes have long been known to produce oscillatory groundwater fluctuations even at large teleseismic distances (Blanchard and Byerly, 1935; Cooper et al., 1965; Rexin et al., 1962; and more recently Brodsky et al., 2003; Kitagawa et al., 2006; Shih, 2009; Wang and Manga, 2010; and many others). In the mid-1900s, when seismograph networks were uncommon, the U.S. Coast and Geodetic Survey kept a detailed catalog of water wells with analog recorders that were good hydroseismographs. Papers were written describing how to construct hydroseismographs and how to locate epicenters and estimate earthquake magnitudes from water well records (e.g., Vorhis, 1965). Ironically, the situation is reversed today. Networks of high quality broadband seismographs cover much of the world while most conventional water well recorders, though digital, are set to take measurements several orders of magnitude too slowly for comprehensive comparison with seismic shaking. Nonetheless, we claim it is possible to extract a reasonable assessment of aquifer specific storage even from well records like that shown in Fig. 1, with a full minute between water level measurements during the passage of the seismic Rayleigh wave.

Accurate aquifer storage estimates are essential for proper groundwater resource evaluation and management. Unlike storage estimates from most well tests, specific storage estimates derived from seismic Rayleigh waves are the result of basin-wide stress. The aquifer as a whole oscillates in volume as these high-amplitude, long-period waves pass.

Seismological theory predicts that while a seismic Rayleigh wave of wavelength λ_k is passing, the relation between the vertical ground displacement and subsurface dilatation in homogeneous media within a few hundred meters of the earth's surface is given by

$$\Delta_k = -1.836\pi\ W_k/\lambda_k. \tag{1}$$

Here Δ_k is the amplitude of the dilatation, and W_k is the amplitude of vertical displacement of the Rayleigh wave of wavelength $\lambda_k \gg z$ where z is the depth of the aquifer (Cooper et al., 1965; Shih, 2009; Stein and Wysession, 2003).

For a uniformly porous confined aquifer, dilatation (the change in aquifer volume per unit volume) can be expressed in terms of specific storage S_s and water level change in an open borehole:

* Corresponding author. Tel.: +1 208 885 6192.
E-mail addresses: attila.folnagy@vandals.uidaho.edu (A.J.B. Folnagy), osiensky@uidaho.edu (J.L. Osiensky), daisuke@vandals.uidaho.edu (D. Kobayashi), ksprenke@uidaho.edu (K.F. Sprenke).

0022-1694/$ - see front matter © 2013 Elsevier B.V. All rights reserved.
http://dx.doi.org/10.1016/j.jhydrol.2013.08.037

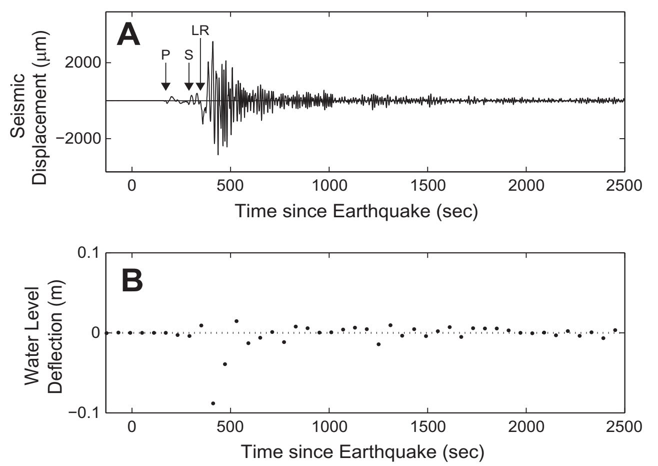

Fig. 1. (A) The M7.5 Haida Gwaii Earthquake. Vertical ground displacement at municipal well M9 in Moscow, Idaho based on regional seismograph station BRAN. The Rayleigh wave arrives at the time indicated by LR and continues across the record. (B) Water level changes driven by the Rayleigh wave as sampled measured at 1-min intervals by a Solinst Levelogger® Gold data logger well recorder.

$$\Delta_k = -S_s H_k / R_k. \tag{2}$$

H_k is the amplitude of the water level oscillation and R_k is the borehole amplification factor (Cooper et al., 1965). As illustrated in the example shown in Fig. 2, this amplification factor is a function of the oscillation frequency. However, it also depends on borehole radius, initial height of the water column, transmissivity of the aquifer, screened aquifer thickness, and, to a minor extent, specific storage (Bredehoeft, 1967). In uniformly porous media, the borehole response can be estimated using the following formula (Cooper et al., 1965):

$$R_k = \left[\left(1 - \{\pi r^2/T\tau\}\mathrm{Kei}\,\alpha - 4\pi^2 H_e/\tau^2 g\right)^2 + \left(\{\pi r^2/T\tau\}\mathrm{Ker}\,\alpha\right)^2\right]^{-1/2}. \tag{3}$$

In this equation, $\alpha = r(\omega S_s b/T)^{1/2}$, r is the radius of the borehole, τ is wave period, ω is angular frequency of the wave, S_s is the specific storage, b is the screened aquifer thickness, T is the transmissivity, H_e is the effective height of the water column, and g is the gravitational acceleration. Ker and Kei are Kelvin functions of the second kind of order zero.

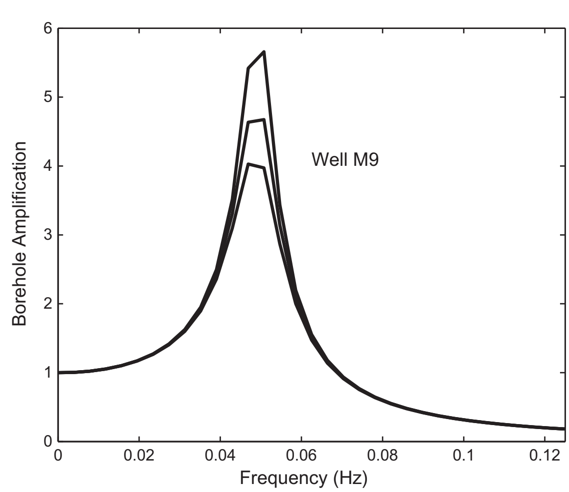

Fig. 2. The borehole response R_k of municipal well M9 in Moscow, Idaho for aquifer storativity estimates of 10^{-3} (upper curve), 10^{-4} (middle curve), and 10^{-5} (lower curve).

Combining Eqs. (1) and (2), one obtains, in theory, a connection between the water level oscillation in the borehole and the Rayleigh wave displacement on the surface:

$$H_k = (1/S_s)(5.77 R_k W_k/\lambda_k). \tag{4}$$

However, in practice, the situation is not so simple. With the exception of S_s, all the variables in the above equation are functions of frequency (as indicated by the subscript k). In practice, spectral methods need to be employed to transform the Rayleigh wave displacements and the water level fluctuations into their constituent frequency components to get useful results. Shih (2009), for example, used the cross spectral density of the two data sets to identify a narrow frequency band of highest coherence. Then, neglecting any borehole effects, the spectral densities and seismic wavelength at that narrow frequency band only were used to calculate the specific storage. The key to Shih's method was having complete spectra of both time series available so that the most coherent period could be identified.

However, accurate spectral methods require measurements of water levels on a time scale similar to that of seismograph data (more than one measurement per second). Such head measurements are rarely obtained (Brodsky et al., 2003; Woodcock and Roeloffs, 1996), making impractical the direct application of spectral methods in most water wells. However, about fifteen moderately large earthquakes (magnitude 7+) occur each year, each producing very high amplitude surface waves for tens of minutes after the shocks. From a statistical viewpoint, these result in a significant amount of data with which to work even if the water levels are only measured every few minutes or so. In this study, we propose an algorithm to use water levels measured minutes apart during the passage of Rayleigh waves, combining measurements from multiple earthquakes if necessary, for the assessment of aquifer specific storage.

2. Computation procedure

2.1. Theory

We assume a uniformly porous confined aquifer penetrated by an open water well. We first consider the problem of roughly estimating specific storage from a single instantaneous water level deflection measurement while a Rayleigh wave segment passes. If this can be accomplished in an unbiased manner, the mean of many such estimations should yield a specific storage to a precision dependent on the number of water level measurements available. The Rayleigh wave segment, consisting of displacements $w(t)$, is represented as the time sequence $w = \{w_0, \ldots, w_{n-1}\}$. This is a discrete sequence of N measurements taken at a constant sampling interval during the passage of a Rayleigh wave segment associated in time with a single instantaneous water level deflection measurement h_i. The discrete Fourier transform of time sequence w is given by:

$$W_k = \sum_{n=0}^{N-1} w_n e^{-i2\pi kn/N}, \tag{5}$$

where $k = 0, 1, 2, \ldots, N-1$, such that the frequency of W_k is k/N cycles per sample interval.

The power spectra of time sequence w is, by definition, given by

$$WW_k = W_k W_k^*/N, \tag{6}$$

where the * operator means complex conjugate. After multiplying each side of (4) by its complex conjugate, and dividing by N, the following equation predicts the power spectra HH_k of the water level oscillations forced by the seismic displacements.

$$HH_k = (1/S_s^2)(33.3 R_k^2/\lambda_k^2) WW_k. \tag{7}$$

It is interesting to note that the adjustment ($33.3\ R_k^2/\lambda_k^2$) created by the wavelength and the borehole response not only enhances oscillations near the resonant frequency of the borehole but also reduces the influence of the longer wavelength (and typically higher amplitude) Rayleigh waves on the water level oscillations.

2.2. Dealing with sparse data

Because the water level data are collected at time intervals much longer than the oscillation periods of the water fluctuations, the measurements are aliased. Thus, the spectrum of the sparse water deflection measurements is an aliased power spectrum. However, for any band-limited signal, the autocorrelation at zero lag (equal to the mean power) is unaffected by aliasing (Passarelli et al., 1984). Therefore, the following relation holds between the aliased water fluctuation measurements $\{h_0, h_1, \ldots, h_{N-1}\}$ and the unaliased power spectrum HH_k of Eq. (7):

$$\frac{1}{N'}\sum_{i=0}^{N'-1} h_i^2 = \frac{1}{N}\sum_{k=0}^{N-1} HH_k, \tag{8}$$

where N' is the number of aliased water deflection measurements. Parseval's theorem relates the squared values of a time sequence to its power spectrum as follows:

$$E\{h^2\} = \frac{1}{N}\sum_{k=0}^{N-1} HH_k. \tag{9}$$

Here, the expected value operator E represents the average of all possible values that the water level deflection h^2 can take on during the passage of the Rayleigh wave segment w. It is important to note that the instantaneous measurement h_i is a single realization of the random variable h. Substituting (7) into (9), one finds that the expected value $E\ \{h^2\}$ of the squared water level fluctuation can be predicted from the mean value of the seismic power spectrum after adjustment for wavelength and borehole effects. That is,

$$E\{h^2\} = (1/S_s^2)E\{(33.3\ R_k^2/\lambda_k^2)WW_k\}. \tag{10}$$

Rearranging (10), the term involving specific storage is given by the ratio of the mean squared water level deflection to the adjusted mean seismic power during the passage of the Rayleigh wave segment.

$$(1/S_s^2) = E\{h^2\}/E\{(33.3\ R_k^2/\lambda_k^2)WW_k\}. \tag{11}$$

Because our quantity to be determined, S_s, is involved in the calculation of the borehole amplification factor R_k, the above equation requires an iterative procedure for its solution. An initial guess of S_s is used to generate successively better approximations. However, because S_s has only a minor effect on R_k, convergence is quickly obtained.Because the water level data are sparse, for any given Rayleigh wave segment, $E\{h^2\}$ is not known. The only estimate available is the single instantaneous value h_i. Nonetheless, for each water level measurement available, the associated Rayleigh wave segment can be processed to get an independent estimate of ($1/S_s^2$) by setting $E\{h^2\} \approx h_i^2$.

$$\left(\frac{1}{Ss^2}\right)_i = \frac{h_i^2}{E\{(33.3\ R_k^2/\lambda_k^2)WW_k\}_i}. \tag{12}$$

Here, the value in the denominator is the mean of an appropriately filtered power spectrum of seismic Rayleigh wave displacement during a time interval associated with the time of water level measurement h_i. We used the Rayleigh wave segment from 75 s before to 75 s after each water level observation to compute the filtered power spectra (Fig. 3). This time interval keeps the seismic spectral estimator as close as possible to the water level measurement time but still long enough to cover the entire frequency range of earthquake Rayleigh waves which can have periods as long as 150 s.

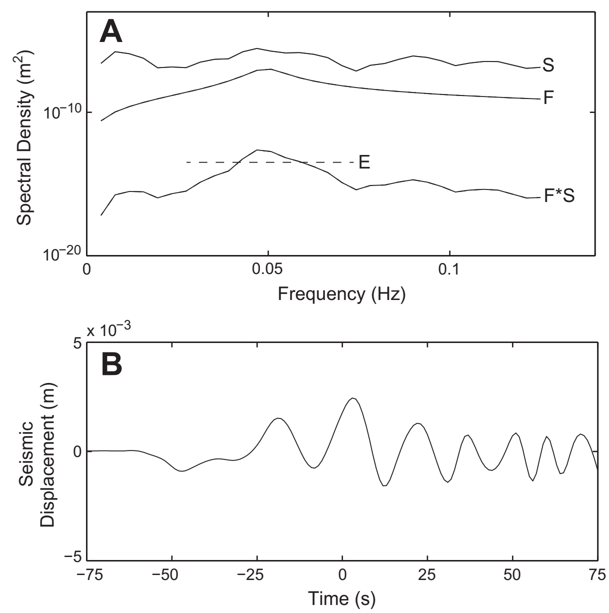

Fig. 3. (A) The plot designated as S is the power spectrum WW_k of the Rayleigh wave segment. Plot F is the filter ($33.3\ R_k^2/\lambda_k^2$) used to adjust the spectrum for borehole amplification and wavelength. Plot F * S is the filtered power spectrum. Level E is at the expected value (mean) of the filtered power spectrum. (B) The 150-s segment of the Rayleigh wave (Fig. 1) for the Haida Gwaii Earthquake centered about the water level measurement 410 s after the origin time. Note that the seismic data in the segment shown have been filtered to remove noise above 0.125 Hz whereas the data shown in Fig. 1 have not.

A considerable number of water measurements and associated Rayleigh wave segments are required to get a reasonable estimate of ($1/S_s^2$). However, because the Rayleigh wave spectrum is calculated independently for each water level measurement, results from multiple earthquakes can be combined until an adequate estimate of ($1/S_s^2$) is obtained.

We use the number (N') of water level measurements available to compute our final value of ($1/S_s^2$), which is simply the arithmetic mean of our estimates:

$$1/Ss^2 = \frac{1}{N'}\sum_{i=1}^{N'} 1/Ss_i^2. \tag{13}$$

The new estimate of specific storage is then the inverse square root of ($1/S_s^2$). This value is then used to recalculate R_k and the entire procedure above is iteratively repeated until a final value of S_s is found that matches the value used in the calculation of R_k.

The usual formula for standard error of the mean can be used to estimate the precision of the computation procedure (not including uncertainties in the input parameters):

$$\mathrm{SEM} = s/N'^{1/2}, \tag{14}$$

where s is the standard deviation of the ($1/S_s^2$) estimates, and N' is the number of water level observations. Clearly, the more water level observations with associated Rayleigh wave segments available, the better the estimate of specific storage by this algorithm. Given a sufficient number of such discrete observations, specific storage can be computed to the same accuracy as can be found from continuous well records.

3. Results

3.1. Simulated data

For the proposed computation procedure to work, the individual values of $(1/S_s^2)_i$ estimated from the discrete water level observations h_i need to be unbiased so that their average, given enough estimates, approaches an accurate value of $1/S_s^2$. To test the algorithm, the process was simulated many times for hypothetical confined uniformly porous aquifers with fixed values of S_s. For each simulation, random synthetic seismograms of Rayleigh wave displacements were used in Eq. (4) to predict the complete sequence h of associated water level oscillations. Then we attempted the inverse problem of recovering the fixed value of S_s using limited numbers of discrete instantaneous measurements h_i.

First, to ensure that aliasing is not a problem, we investigated the effect of sample interval on the proposed computation procedure. We started with a simulated 4 h long water level recording at the same interval as the unaliased seismic results. To do this, we repeatedly generated a random Rayleigh wave train 4 h long and band-limited to the frequency range of Rayleigh waves from natural earthquakes (0.00667–0.125 Hz). We then computed its Fourier transform, W_k, using Eq. (5), and then calculated the complete unaliased water level time sequence, h, using Eq. (4) with typical values for R_k and λ_k and the fixed value of S_s. We then undersampled h at increasing time intervals to assemble sequences $\{h_0, h_1, h_2, \ldots\}$ of simulated measurements at each sampling rate. We followed the procedure outlined above to obtain an S_s estimate using Eq. (13) for comparison to the fixed value. The mean and 68% confidence limits of 1000 simulations at each sampling interval are shown in Fig. 4A. The bias, after 1000 simulations, increases from less than 1% for the unaliased signal to only about 3% for the highly aliased sampling interval of 10 min. The precision of the algorithm, as measured by the standard error, increases from near zero at the lowest sampling interval to about 14% at the 10 min sampling interval.

To isolate the effects of aliasing, we repeated the simulations above but sampled each signal only 240 times at each sample interval. In this case, in contrast to Fig. 4A, the bias and standard error are essentially independent of the sample interval (Fig. 4B). Thus, as predicted by theory, aliasing has little effect on the simulated results. The small increase in bias and the larger increase in standard error apparent in Fig. 4A is not the result of aliasing, but simply because, for a signal of constant length, fewer measurements are averaged at the longer sampling intervals.

Fig. 4C is like Fig. 4A but with number of measurements, instead of sample interval, on the abscissa. In all cases simulated, the estimated S_s values converge, in accordance with Eq. (14) toward the fixed value of S_s as the number of measurements increase. These simulations not only show that the computation procedure, given enough measurements, is accurate in principle, but also give an idea of the number of water level measurements required to achieve a required level of computational precision. After 60 measurements, regardless of the sampling interval, the standard error is about 10% of the fixed value of S_s. After about 240 measurements, the standard error is about 5% of the fixed value. About 1000 measurements would reduce the standard error of the computation procedure to near 1%.

The point of the simulations was to show that the computation procedure is unbiased. Assuming all initial assumptions are satisfied, it will in fact recover the correct value of specific storage given sufficient discrete measurements of water levels during the passage of Rayleigh waves. Other algorithms, such as solving for S_s directly instead of $1/S_s^2$ at each data point in Eq. (12) or of using the median instead of the mean in Eq. (13), failed to recover the correct

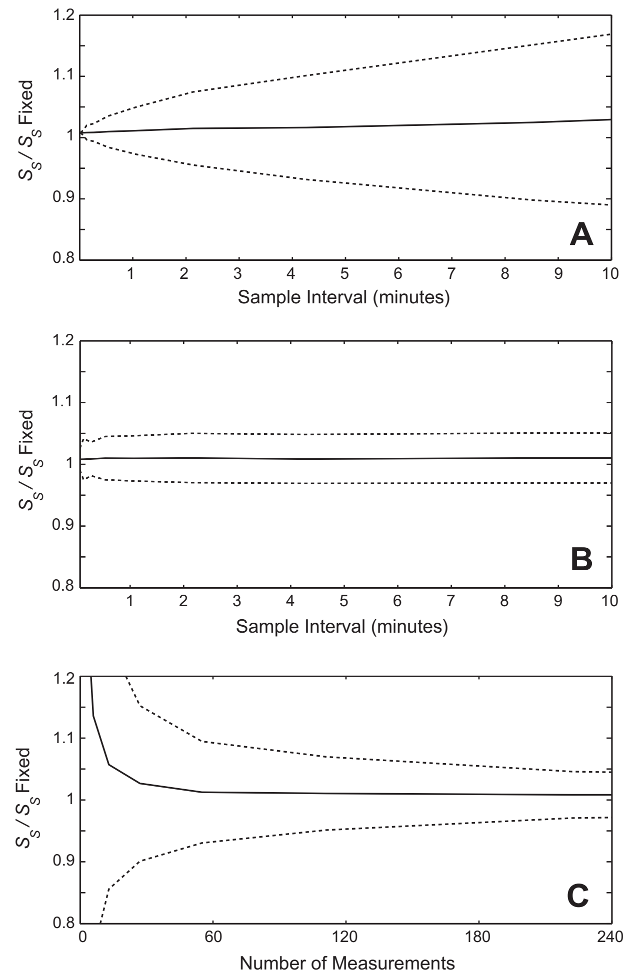

Fig. 4. The mean (solid line) and 68% confidence limits (dashed lines) of specific storage estimates from 1000 simulated water level recordings for a fixed value of S_s, but aliased at increasing sample intervals: (A) For the case of water level records of constant length (4 h). (B) For the case of water level records of different lengths but with the same number of measurements (240). (C) As in A, but plotted against number of measurements.

fixed value of specific storage in simulations. We did many simulations with randomly generated synthetic seismograms, well responses, and specific storage values to show that the error in the computation procedure is controlled by the number of available water level measurements.

3.2. Simulations with noise

To test the robustness of our algorithm, we performed additional simulations with different amounts of random noise added to the seismic signal. Noise in the seismic signal will bias the resulting specific storage estimate to higher values. The results are shown in Fig. 5. At a totally "swamped" signal to noise ratio (SNR) of 0 dB (noise amplitude equal to signal amplitude) our proposed computation procedure produces a specific storage estimate biased by 35%. At an SNR of 6 dB (noise amplitude half of signal amplitude), the bias in Ss drops to less than 5%. At an SNR of 20db (noise amplitude 10% of signal amplitude), the bias drops to less than 1%. Thus, our proposed algorithm is reasonably robust, at least against random white noise in the seismic signal. Noise in the water level measurements would have similar effects except the bias would be toward lower values of specific storage, possibly

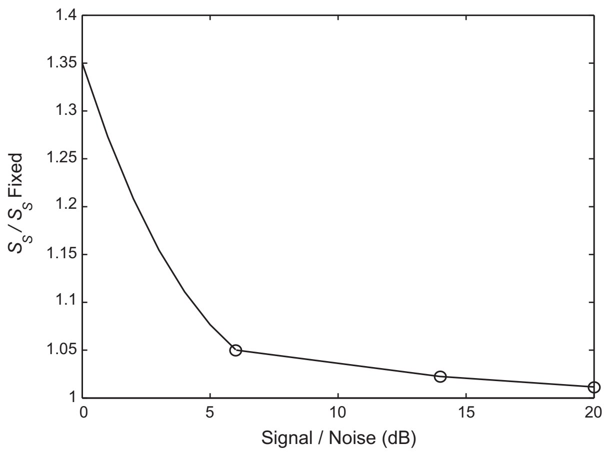

Fig. 5. The mean of specific storage estimates from 1000 simulated water level recordings for a fixed value of S_s in the presence of white noise in the seismic signal.

working against any noise in the seismic signal. Nonetheless, because the algorithm allows the use of data from multiple earthquakes, it would be worthwhile to selectively use events with clean seismic and water level records.

3.3. Real data

To apply the method to a particular well, one requires many discrete measurements of water level deflections taken during the passage of seismic Rayleigh waves. Measurements from many different earthquake events can be combined and used. Also required are segments, 150 s in duration, of the Rayleigh wave displacement seismogram spanning the time of each water level fluctuation measurement. Also necessary is knowledge of Rayleigh wave phase velocities in the region so that the wavelength (phase velocity $\times$ period) can be calculated at each frequency for the required adjustment. These phase velocity data are available in the seismological literature. Also required are knowledge of the borehole geometry and a good prior estimate of transmissivity.

As an example of our method, we evaluated the Rayleigh wave response of municipal well M9 in Moscow, Idaho, in the northwestern United States. This important supply well was shut down temporarily for pump repair for several months in 2012, giving an opportunity for the installation of a Solinst Levelogger® Gold data logger. The well is cased except for 27 m of screen adjacent to several interconnected highly permeable flow top units within the Grande Ronde aquifer. The top of the aquifer is at a depth of 198 m. The static level of the water rises to a height of 104 m above the top of this confined artesian aquifer. The borehole diameter above the screened intervals is 0.22 m. The barometric efficiency of the well is 0.97. Previous well tests indicated a transmissivity of about 18,000–21,000 m^2/day and a storativity on the order of 10^{-4} (McVay, 2007).

Rayleigh waves from three moderately large earthquakes were studied (Table 1). The Pacific Northwest Seismograph Network (PNSN) University of Washington regional broadband station in Enterprise, Oregon (BRAN) was the closest station to well M9. The facilities of the IRIS Data Management Center were used for access to the waveforms for this event from regional broadband seismograph stations. Seismic data were downloaded from IRIS using the Java program JWEED. The vertical broadband velocity data initially recorded at 40 Hz were low-pass filtered to remove frequencies above 0.125 Hz, decimated to a one second sampling interval, corrected for instrument response, and then integrated to yield vertical ground displacement.

The USGS National Earthquake Information Center provides a very useful "Earthquake Travel Time Information and Calculator" on their website, which was used to determine epicentral distances and phase arrival times at the M9 well and at station BRAN. The record of vertical ground displacement at M9 for the Haida Gwaii earthquake is shown in Fig. 1A. The Rayleigh wave is preceded by the P-wave and S-wave phases. We extracted the displacements for 4096 s beginning with the first arrival of the Rayleigh wave. We then further filtered the data, removing any noise above 0.125 Hz.

During the same time intervals as the Rayleigh wave arrivals, the data logger in well M9 was collecting measurements at 1 min intervals (Fig. 1B). By inspection of the water level records, we chose to use 20 water level measurements immediately after the Rayleigh wave first arrival for each of three separate earthquakes. The water level fluctuations from the base line were tabulated and squared. As illustrated in Fig. 3, we associated with each water level data point a Rayleigh wave segment beginning 75 s before and ending 75 s after the water level measurement. The power spectrum WW_k of each Rayleigh wave segment was calculated individually. The velocity dispersion curve for the western United States (Yang and Forsyth, 2006) was used to derive the wavelengths λ_k required.

For each water level measurement, an estimate of $(1/S_s^2)_i$ was then made using Eq. (12). These results, after the final iteration of the algorithm, are plotted in Fig. 6 for each earthquake. The abscissa of this plot is the time of the water measurements after the initial arrival of the Rayleigh wave train for each seismic event. We plotted the data in this manner to look for evidence of noise. As can be seen in Fig. 1, Rayleigh waves begin with high amplitudes that gradually fade. It is reasonable to expect that the SNR of the Rayleigh wave data will decrease with time on the seismogram. However, at least in the first 20 min of the Rayleigh wave of which we made use, there is no correlation of the $(1/S_s^2)_i$ estimates with arrival time.

Table 1
Seismological information.

Earthquake	Haida Gwaii	Philippine	Okhotsk
Date[a]	October 27, 2012	August 31, 2012	August 14, 2012
Magnitude[a]	M_W 7.8	M_W 7.8	M_W 7.7
Location[a]	52.781°N 132.103°W	10.838°N 126.704°E	49.784°N, 145.126°E
Depth[a]	20 km	35 km	626 km
Origin time[a]	03:04:09 UTC	12:47:34 UTC	02:59:42 UTC
Delta (BRAN)	11.84°	99.63°	60.95°
Delta (M9)	11.46°	99.41°	60.54°
LR group velocity	$3.51 \times 10^{-2}\ s^{-1}$	$3.55 \times 10^{-2}\ s^{-1}$	$3.55 \times 10^{-2}\ s^{-1}$
LR arrival time (BRAN)	03:09:47 UTC	13:34:20 UTC	03:28:18 UTC
LR arrival time (M9)	03:09:36 UTC	13:34:14 UTC	03:28:07 UTC
Geometric spreading correction[b]	1.016	1.001	1.003

[a] Data from USGS National Earthquake Information Center.
[b] $(\text{Delta\_BRAN}/\text{Delta\_M9})^{0.5}$.

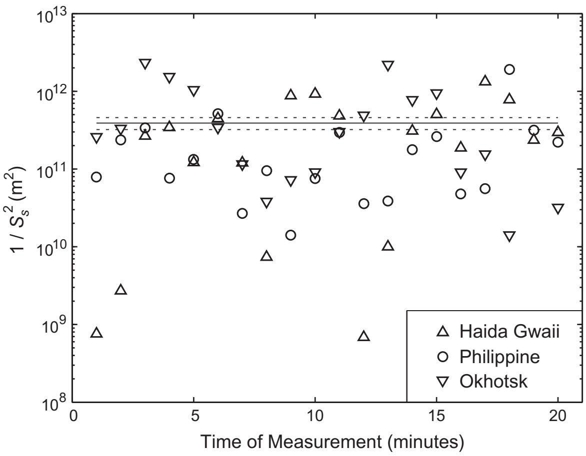

Fig. 6. Individual estimates of $1/S_s^2$ based on instantaneous water fluctuation measurements made at the time indicated after the initial arrival of the Rayleigh wave train for each seismic event. The mean (solid line) and its 68% confidence intervals on the mean (dashed lines) are also shown.

The mean $1/S_s^2$ and 68% confidence intervals on the mean as calculated by Eqs. (13) and (14) are also shown in Fig. 6. Our final estimate of S_s is 1.5×10^{-6} m^{-1}. The standard error of this value is about 10%, a computational precision consistent with our simulation results (Fig. 4C) for the case of 60 water level measurements.

The error due to our computation procedure is comparable to other quantitative sources of error inherent in the method. Our value of transmissivity used in the borehole response function has an uncertainty of 15%, resulting in an uncertainty of about 7% in S_s. Well M9 is a long way (160 km) from the nearest regional broadband stations. Based on interpolations from several seismic stations, we estimate that our uncertainty in Rayleigh wave displacement is about 6% at M9. This translates to an uncertainty in the derived S_s of 8%. The above sources of error being largely independent, our best estimate of S_s is $1.5 \pm 0.2 \times 10^{-6}$ m^{-1}. However, this optimistic figure does not take into account sources of error that are difficult to quantify. The method assumes the aquifer is confined, uniformly porous, and free of heterogeneities. As with any aquifer stress test, uncertainties in these assumptions probably outweigh the calculated standard errors.

Specific storage is poorly known for the Grande Ronde aquifer as a whole. Previous estimates based on pump tests, barometric efficiency, and analytic modeling range over four orders of magnitude. However, an analysis of earth tide response in a Grande Ronde aquifer observation well several miles from M9 (Sprenke et al., 2011) did result in an S_s of 1.44×10^{-6} m^{-1}, a value in excellent agreement with our result.

4. Discussion

This method is applicable only for water wells in confined aquifers of known transmissivity which behave as predicted by seismological and well hydraulics theory for uniformly porous media. Some wells are poorly constructed which inhibits flow into or out of the borehole (e.g., Cooper et al., 1965; Liu et al., 1989). In other aquifers, seismic shaking, even at teleseismic distances, is sufficient to alter permeability either permanently or cyclically perhaps by liquefaction, fracture blocking, air bubble growth (e.g., Brodsky et al., 2003; Elkhoury et al., 2006; Linde et al., 1994; Roeloffs, 1998). In some aquifers (perhaps even the Grande Ronde aquifer studied in this paper), a fracture flow model (e.g., Brodsky et al., 2003) might be more relevant. In these complex situations, water levels should be measured on the order of seconds, not minutes, if meaningful synthesis with Rayleigh wave displacement is to be accomplished and the details of the groundwater model revealed.

5. Conclusions

Because high quality regional seismological data are now freely available in digital form for most areas of the world, the method proposed here could prove to be a valuable tool to complement and validate aquifer storage estimates from more conventional methods.

Any major discrepancy would suggest that some assumption about the aquifer model is incorrect – perhaps revealing the aquifer to be partially unconfined, heterogeneous or anisotropic. A major advantage of the method is that the entire aquifer is stressed almost simultaneously by the long wavelength Rayleigh waves, quite unlike the localized stress field associated with most pump tests. A further advantage of the method is its logistical simplicity. Because of the statistical nature of the measurements involved, the well recorders do not have to be particularly sophisticated. As long as the timing is accurate to better than 1 min and measurements are recorded on the order of minutes, a reasonable estimate of the mean-squared oscillatory fluctuation during the passage of the Rayleigh wave should be obtainable, especially because the method allows the results from many earthquakes to be combined.

Acknowledgments

We thank Niklas Linde and five anonymous reviewers whose comments have greatly improved this manuscript. We also thank the Palouse Basin Aquifer Committee (PBAC) for providing partial funding, Steve Robischon of PBAC for collecting and providing the water level data, and the Pacific Northwest Seismic Network at the University of Washington for the seismic data. The IRIS DMS is funded by the people of the United States of America through the Instrumentation and Facilities Program of the National Science Foundation.

References

Blanchard, F.B., Byerly, P., 1935. A study of a well gauge as a seismograph. Bull. Seismol. Soc. Am. 25 (4), 313–321.
Bredehoeft, J.D., 1967. Response of well-aquifer systems to Earth tides. J. Geophys. Res. 72 (12), 3075–3087.
Brodsky, E.E., Roeloffs, E., Woodcock, D., Gall, I., Manga, M., 2003. A mechanism for sustained groundwater pressure changes induced by distant earthquakes. J. Geophys. Res. 108 (B8), 2390.
Cooper Jr., H.H., Bredehoeft, J.D., Papadopulos, I.S., Bennett, R.R., 1965. The response of well-aquifer systems to seismic waves. J. Geophys. Res. 70 (16), 3915–3926.
Elkhoury, J.E., Brodsky, E.E., Agnew, D.C., 2006. Seismic waves increase permeability. Nature 441, 1135–1138.
Kitagawa, Y., Koizumi, N., Takahashi, M., Matsumoto, N., Sato, T., 2006. Changes in groundwater levels or pressures associated with the 2004 earthquake off the west coast of northern Sumatra (M9.0). Earth, Planets Space 58 (2), 173–179.
Linde, A.T., Sacks, I.S., Johnston, M.J.S., Hill, D.P., Bilham, R.G., 1994. Increased pressure from rising bubbles as a mechanism for remotely triggered seismicity. Nature 371, 408–410.
Liu, L.-B., Roeloffs, E., Zheng, X.-Y., 1989. Seismically induced water level fluctuations in the Wali Well, Beijing. China. J. Geophys. Res. 94 (B7), 9453–9462.
McVay, M., 2007. Grande Ronde aquifer characterization in the Palouse Basin. MSc Thesis, Department of Geological Sciences, University of Idaho, Moscow, ID.
Passarelli Jr., R.E., Serafin, R.J., Strauch, R.G., 1984. Effects of aliasing on spectral moment estimates derived from the complete autocorrelation function. J. Clim. Appl. Meteorol. 23 (5), 848–849.
Rexin, E.E., Oliver, J., Prentiss, D., 1962. Seismically-induced fluctuations of the water level in the Nunn-Bush well in Milwaukee. Bull. Seismol. Soc. Am. 52 (1), 17–25.
Roeloffs, E.A., 1998. Persistent water level changes in a well near Parkfield, California, due to local and distant earthquakes. J. Geophys. Res. 103 (B1), 869–889.
Shih, D.C.-F., 2009. Storage in confined aquifer: spectral analysis of groundwater responses to seismic Rayleigh waves. J. Hydrol. 374 (1–2), 83–91.

Sprenke, K.F., Folnagy, A.J., Osiensky, J.L., 2011. Aquifer Storage from Sparse Records of Groundwater Response to Large Earthquakes. AGU Fall Meeting Abstracts, vol. 1, p. 1389.
Stein, S., Wysession, M., 2003. An Introduction to Seismology, Earthquakes, and Earth Structure, first ed. Wiley-Blackwell, New Jersey.
Vorhis, R.C., 1965. Earthquake magnitudes from hydroseismic data. Groundwater 3 (1), 12–20.
Wang, C.-Y., Manga, M., 2010. Earthquakes and Water. Springer-Verlag, Berlin, 225 p.
Woodcock, D., Roeloffs, E.A., 1996. Seismically induced water-level oscillation in a fractured-rock aquifer well near Grants Pass, Oregon. Oregon Geol. 58, 27–33.
Yang, Y., Forsyth, D.W., 2006. Rayleigh wave phase velocities, small-scale convection, and azimuthal anisotropy beneath southern California. J. Geophys. Res. 111 (B7), B07306.